Electronic Supplementary Information (ESI) for Soft Matter

Prediction of polydisperse hard-sphere mixture behavior using tridisperse systems

Vitaliy Ogarko,[*a] **and Stefan Luding**[a]

1 Details on the Event-driven Molecular Dynamics (EDMD) simulations

In our EDMD simulations we used a modification of the Event-Driven C++ code written by A. Donev *et al.*[1,2], which is available for download at `http://cherrypit.princeton.edu/Packing/C++/`.

In our work we consider, in the style of A. Donev[3], Molecular Dynamics in a simple bounded simulation domain embedded in a Euclidean space of dimensionality d, defined by the *lattice vectors*, $\boldsymbol{\lambda}_1$,..., $\boldsymbol{\lambda}_d$. The simulation domain, or unit cell, is a collection of points with d *relative coordinates* $\mathbf{r}$ in the interval [0,1], and corresponding Cartesian coordinates

$$\mathbf{r}^{(E)} = \sum_{k=1}^{d} r_k \boldsymbol{\lambda}_k = \boldsymbol{\Lambda}\mathbf{r}, \tag{1}$$

where $\boldsymbol{\Lambda}$ is a square invertible matrix representing the lattice, and contains the lattice vectors as columns. The volume of the unit cell is given by the positive determinant $V \equiv |\boldsymbol{\Lambda}|$. In particular, we consider a *cubic* unit cell in 3D (d=3) with lattice vectors $\boldsymbol{\lambda}_1 = (1,0,0)$, $\boldsymbol{\lambda}_2 = (0,1,0)$ and $\boldsymbol{\lambda}_3 = (0,0,1)$.

Additionally, we use periodic boundary conditions (BCs) which are imposed to mimic an infinite system, i.e., a statistically homogeneous medium. One can interpret periodic systems as being "infinite" and covering all Euclidean space with identical copies of the unit cell and the particles in this unit cell, however the system size $\boldsymbol{\lambda}_k$ defines the minimum possible wavenumber (largest wavelength). Periodic BCs are handled by considering the unit cell of the packing and considering each contact between an original i and an image particle $\tilde{j}$ to be a contact between particles i and j. The vector of d integers $\mathbf{n}_{ij}$ specifies how many unit cells the contact $\{i, j\}$ crosses over[3]. This way the relative position between particles i and j is

$$\mathbf{r}_{ij} = \mathbf{r}_i - \mathbf{r}_j + \boldsymbol{\Lambda}\mathbf{n}_{ij}, \tag{2}$$

with the positions $\mathbf{r}_i$ and $\mathbf{r}_j$ of the centers of particles i and j, respectively.

Given velocities of the particles just before the contact, $\mathbf{v}_1$ and $\mathbf{v}_2$, and their masses m_1 and m_2, the velocities after the collision are derived[4] from conservation of linear momentum and definition of the restitution coefficient, e_n, yielding:

$$\mathbf{v'}_1 = \mathbf{v}_1 + \Delta\mathbf{p}/m_1, \tag{3}$$

$$\mathbf{v'}_2 = \mathbf{v}_2 - \Delta\mathbf{p}/m_2, \tag{4}$$

where $\Delta\mathbf{p}$ is the change of momentum. In the case of smooth (frictionless) particles only the normal component of the change of momentum $\Delta\mathbf{p}^{(n)}$ is affected during the collision (i.e., no angular velocity), and it is calculated as[4]:

$$\Delta\mathbf{p}^{(n)} = -m_{12}(1+e_n)\mathbf{v}_c^{(n)}, \tag{5}$$

[a] *Multi Scale Mechanics (MSM), CTW, MESA+, University of Twente, PO Box 217, 7500AE Enschede, Netherlands; E-mail: v.ogarko@utwente.nl*

with the reduced mass $m_{12} = m_1 m_2/(m_1+m_2)$, and the normal component of the relative velocity of the contact-point of the particles $\mathbf{v}_c^{(n)}$. The latter is calculated taking into account the expanding sphere surfaces (for growing particles) as:

$$\mathbf{v}_c^{(n)} = \hat{\mathbf{n}}\left[(\mathbf{v}_1-\mathbf{v}_2)\cdot\hat{\mathbf{n}} - (v_1^{gr}+v_2^{gr})\right], \tag{6}$$

with the unit vector in the normal direction $\hat{\mathbf{n}} = \mathbf{r}_{ij}/\left\|\mathbf{r}_{ij}\right\|$, and the growing speed of radius a_i of particle i

$$v_i^{gr} := \frac{da_i}{dt} = \Gamma\frac{a_i}{a_{\max}}v_0, \tag{7}$$

where $a_{\max}$ is the largest particle radius at time t, and $v_0 := \sqrt{\frac{2E}{3M}}$ is the thermal velocity, defined via the total fluctuation kinetic energy, E, and the total system mass, M, and Γ is the dimensionless growth (compression) rate.

The compressibility factor $Z \equiv pV/Nk_BT$, with kinetic temperature $k_BT = 2E/3N$, is calculated from the total exchanged momentum in all interparticle collisions during a short time period Δt:

$$Z = 1 - \frac{\sum\left\|\Delta\mathbf{p}_{ij}\right\| l_{ij}}{2E\Delta t}, \tag{8}$$

where the bar $l_{ij} = \left\|\mathbf{r}_{ij}\right\|$ accounts for the distance over which momentum (force) is transmitted. The time period Δt is chosen so that the total change in the kinetic energy due to growth stays below 1%.

To account for stability of the code (numerical errors), we allow particles to have a very small overlap, given by the following expression:

$$\left\|\mathbf{r}_{ij}\right\|^2 - (a_i+a_j)^2 \geq -10^{-12}(a_i+a_j). \tag{9}$$

This way the code does not break down near jamming, even for very high compressibility factor $Z \approx 10^{12}$.

2 Size distribution parameters

In order to facilitate the process of finding a maximally equivalent tridisperse system, we consider, in the style of Bartlett[5], the tridisperse distribution detailed in Table 1. This distribution has been chosen so that varying the number fractions $n_{1,2}$, and the non-dimensional radii weighed by number fractions, $\delta_i = n_i a_i/\langle a\rangle$, $i = 1,2$, allows the mixture composition and volume fraction to change, while the total number density $\rho = N/V$ and mean radius $\langle a\rangle$ are fixed. Note that any tridisperse mixture can be expressed in this form, since this distribution has six degrees of freedom as desired (i.e., $2s$ for $s = 3$ species): ρ, $\langle a\rangle$, $\delta_{1,2}$ and $n_{1,2}$. This is equivalent to the set ν, $\langle a\rangle$, $\langle a^2\rangle$,..., $\langle a^5\rangle$, as used in the paper, and these two sets are related as:

$$\left\langle a^k\right\rangle = \sum_{i=1}^{3} n_i a_i^k = \langle a\rangle^k\left(\frac{\delta_1^k}{n_1^{k-1}} + \frac{\delta_2^k}{n_2^{k-1}} + \frac{(1-\delta_1-\delta_2)^k}{(1-n_1-n_2)^{k-1}}\right), \quad k \geq 1, \tag{10}$$

$$\nu = \rho\frac{4\pi}{3}\left\langle a^3\right\rangle. \tag{11}$$

Consider polydisperse systems with a uniform size distribution of radii (e.g., same number of bigger spheres as smaller spheres in intervals da), characterized by its extreme size ratio $\omega = a_{\max}/a_{\min}$, i.e., the ratio between the maximum and the minimum particle radius. The radius of the particles in such systems is

Table 1 Specification of a tridisperse mixture of hard spheres with fixed values for the total number density of particles, ρ, and mean radius $\langle a \rangle$. The properties of the mixture are then uniquely defined by the variables $\delta_i = n_i a_i / \langle a \rangle$ and $n_i = N_i/N$.

	Species 1	Species 2	Species 3
Number density ρ_i	ρn_1	ρn_2	$\rho(1-n_1-n_2)$
Radius a_i	$\langle a \rangle \dfrac{\delta_1}{n_1}$	$\langle a \rangle \dfrac{\delta_2}{n_2}$	$\langle a \rangle \dfrac{(1-\delta_1-\delta_2)}{(1-n_1-n_2)}$

distributed uniformly between $a_{\min} = (1-\omega_0)\langle a \rangle$ and $a_{\max} = (1+\omega_0)\langle a \rangle$, where $\omega_0 = (\omega-1)/(\omega+1)$, and $2\omega_0 \langle a \rangle = a_{\max} - a_{\min}$ is the width of the (normalized) size distribution function $f(a)$:

$$f(a) = \frac{1}{2\omega_0 \langle a \rangle} \Theta(a_{\max} - a)\Theta(a - a_{\min}), \tag{12}$$

with the Heaviside step function $\Theta(x) = 1$ for $x \geq 0$ and $\Theta(x) = 0$ elsewhere. For the uniform size distribution, due to its simplicity, maximally equivalent systems can be found analytically. We do it by solving a system of four equations that matches the first four central scaled moments with the tridisperse system from Table 1. Central scaled moments are very simple for the uniform size distribution:

$$\begin{aligned} M_2^c &= (1/3)\omega_0^2, \\ M_3^c &= 0, \\ M_4^c &= (1/5)\omega_0^4, \\ M_5^c &= 0, \end{aligned} \tag{13}$$

with $M_1^c = 0$, due to the definition:

$$M_k^c = \frac{\left\langle (a - \langle a \rangle)^k \right\rangle}{\langle a \rangle^k}. \tag{14}$$

Therefore, maximally equivalent tridisperse systems to the uniform size distribution (with parameter ω) can be obtained analytically (e.g., using Mathematica software):

$$n_1 = \frac{5}{18}, \quad n_2 = \frac{8}{18}, \tag{15}$$

$$\delta_1(\omega) = \frac{1}{18}(5 + \sqrt{15}\omega_0), \quad \delta_2 = \frac{8}{18}. \tag{16}$$

Note that here and further we pick a only (unique) solution (for a given ω) with $a_1 \geq a_2 \geq a_3$ (sorted radii). Furthermore, equivalent systems (with matched $k = 2,3,5$ scaled moments) to a system with uniform size distribution with $\omega = 3$, considered in the paper in Figure 1(b), are detailed below for different kurtosis $\beta_2 = M_4^c/(M_2^c)^2$:

$$n_1 = \frac{1}{2\beta_2}, \quad n_2 = \frac{\beta_2 - 1}{\beta_2}, \tag{17}$$

$$\delta_1 = \frac{6 + \sqrt{3\beta_2}}{12\beta_2}, \quad \delta_2 = \frac{\beta_2 - 1}{\beta_2}. \tag{18}$$

Consider systems with uniform volume distribution of radii in the sense that the total volume occupied with those particles with radii between a_1 and $a_1 + da$ is equal to the total volume occupied by particles

with radii between a_2 and $a_2 + da$, etc. These systems can be also characterized by their extreme size ratio $\omega = a_{\max}/a_{\min}$. This is a truncated power law size distribution, which due to its sharp edges with well defined ω, could be obtained by ideal sieving from wider, smooth continuously distributed realistic distributions. Power law distributions appear in a diverse range of natural and man-made phenomena[6]. The radius of the particles in such systems is distributed between $a_{\min} = \frac{\omega+1}{2\omega}\langle a\rangle$ and $a_{\max} = \frac{\omega+1}{2}\langle a\rangle$ and the (normalized) size distribution function $f(a)$ is expressed as:

$$f(a) = \frac{\langle a\rangle^2}{2\omega_0} a^{-3}\Theta(a_{\max} - a)\Theta(a - a_{\min}). \tag{19}$$

Tridisperse maximally equivalent systems to polydisperse ones with uniform volume radii distribution, as considered in the paper in Figure 2, are detailed in Table 2. First four raw scaled moments $M_k = \langle a^k\rangle / \langle a\rangle^k$ for the uniform volume radii distribution are:

$$\begin{aligned} M_2 &= \frac{\ln\omega}{2\omega_0}, \\ M_3 &= \frac{(1+\omega)^2}{4\omega}, \\ M_4 &= \frac{(1+\omega)^4}{16\omega^2}, \\ M_5 &= \frac{(1+\omega)^4(1+\omega+\omega^2)}{48\omega^3}. \end{aligned} \tag{20}$$

To avoid possible confusion, we note that in the distribution detailed in Eq. (19), what is actually uniformly distributed is the inverse area $z = a^{-2}$:

$$f(z)dz = f(a)da, \;\; dz = -2a^{-3}da, \tag{21}$$

therefore, $f(z) = f(a)/(-2a^{-3}) = \text{const}$ for $a_{\max}^{-2} \le z \le a_{\min}^{-2}$. Accordingly, a proper nomenclature for this type of size distribution is *uniform inverse area* distribution (per inverse-area interval). However, we stick to the uniform volume size distribution in the sense defined above Eq. (19), in order to talk about size distributions only.

Table 2 Specification of tridisperse mixtures of hard spheres maximally equivalent to polydisperse systems with uniform volume distribution of radii for various extreme size ratios ω.

ω	n_1	n_2	δ_1	δ_2
2	0.1427	0.4054	0.1988	0.4337
3	0.08923	0.3544	0.1593	0.4181
4	0.06189	0.3118	0.1345	0.4034
5	0.04582	0.2777	0.1173	0.3902
6	0.03548	0.2502	0.1044	0.3785
8	0.02331	0.2086	0.08630	0.3584
10	0.01661	0.1789	0.07400	0.3419

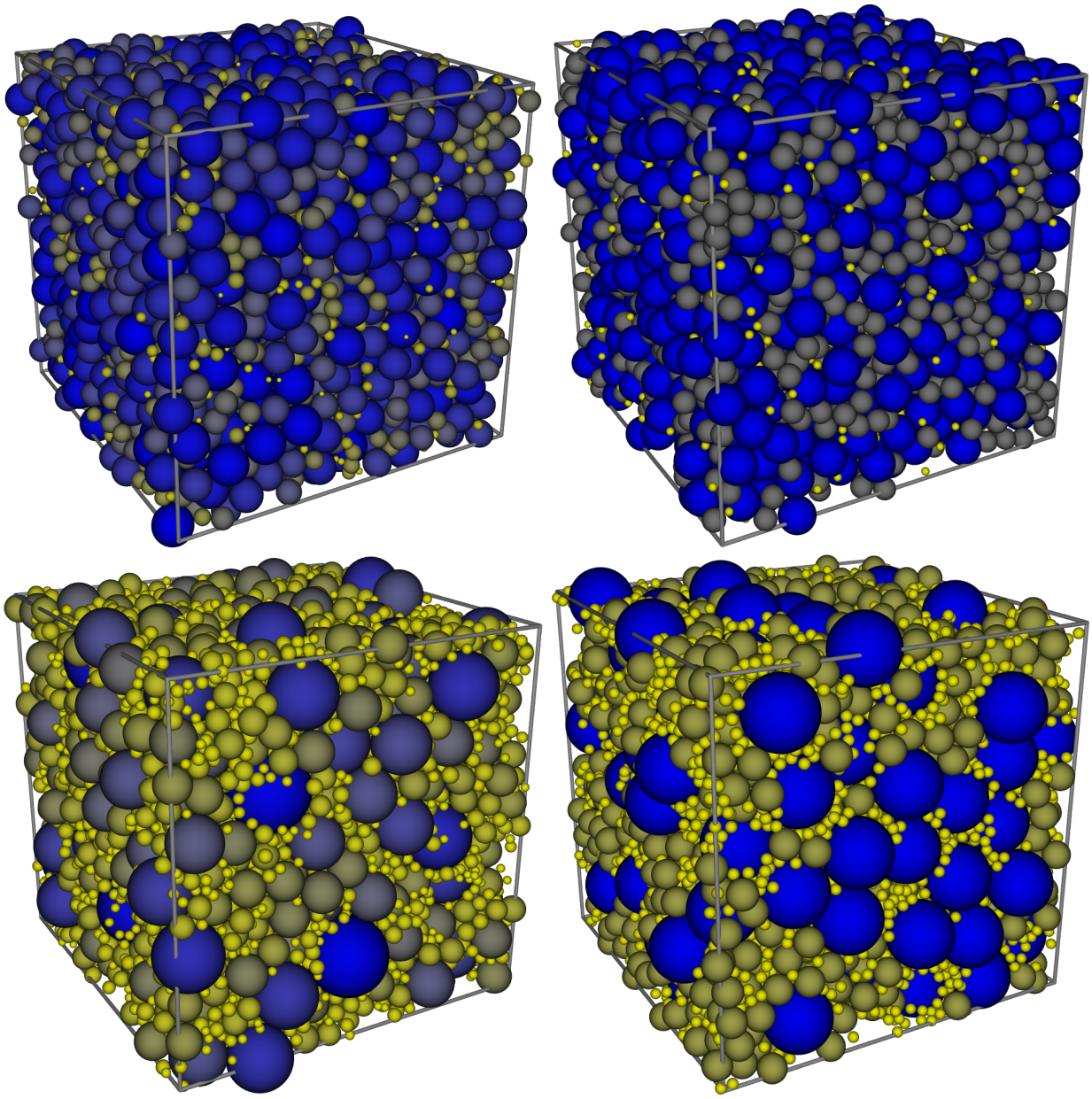

Figure 1 (top left) A polydisperse system with uniform size radii distribution with $\omega = 10$ and $N = 4096$ particles and (top right) its maximally equivalent tridisperse counterpart, and (bottom left) a polydisperse system with uniform volume radii distribution with $\omega = 10$ and $N = 8192$ particles and (bottom right) its maximally equivalent tridisperse counterpart. Color is by relative size, where darker grey particles are bigger – in color blue.

Log-normal distributions appear in studies of emulsions, granular materials, such as sediments[7] and particle growth processes[8]. Therefore, we also study this size distribution of sphere radii, which has the form[7]:

$$f(a) = \frac{1}{\sigma\sqrt{2\pi}a}\exp\left\{-\frac{[\ln(a/a_0)]^2}{2\sigma^2}\right\}, \tag{22}$$

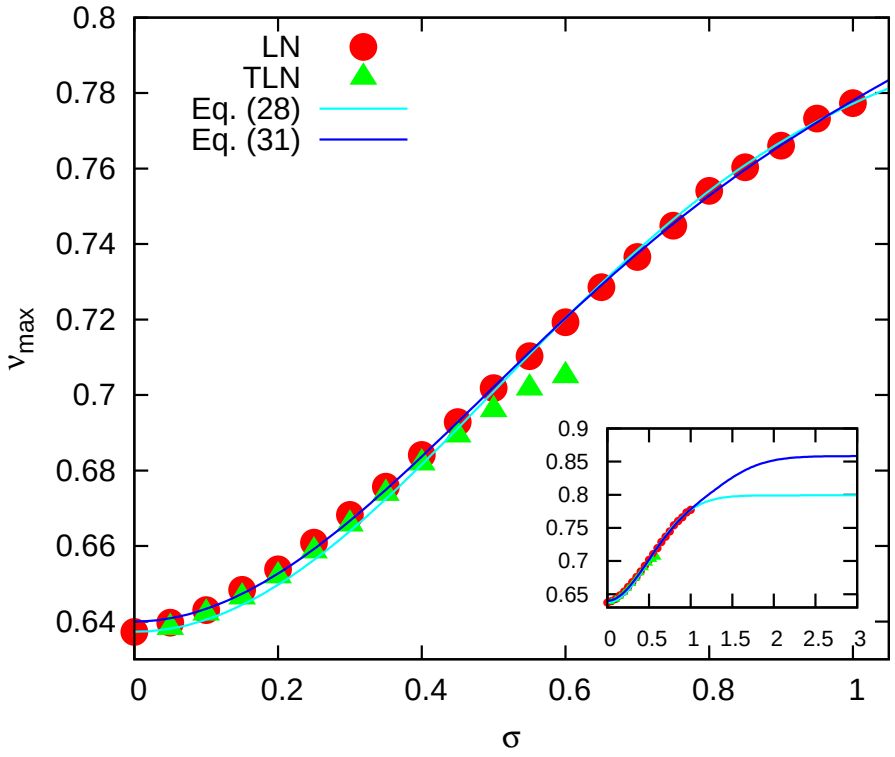

Figure 2 Jamming density plotted against σ for systems with log-normal (LN) radii distribution and for their tridisperse maximal equivalents (TLN), using $N = 16384$. In the inset, the behavior of the fitting equations beyond the range of data is shown for larger values of σ, using the same axis and symbols. The deviation between LN and TLN data is due to the rattler-removed packings have highly different moments and thus being not true maximally equivalent anymore.

where a_0 is a reference radius setting the length scale:

$$a_0 = (1/2)(D_{32}D_{43})^{1/2}(D_{32}/D_{43})^3, \tag{23}$$

and σ is the dimensionless geometric standard deviation:

$$\sigma = \sqrt{\ln\left(\frac{D_{43}}{D_{32}}\right)}, \tag{24}$$

with (often experimentally accessible) the volume-weighted mean diameter D_{43} and the surface-weighted mean diameter D_{32} defined in terms of the moments via:

$$D_{43} \equiv 2\left\langle a^4\right\rangle / \left\langle a^3\right\rangle, \tag{25}$$

$$D_{32} \equiv 2\left\langle a^3\right\rangle / \left\langle a^2\right\rangle. \tag{26}$$

The log-normal moments $\left\langle a^k\right\rangle$ are given by

$$\left\langle a^k\right\rangle = a_0^k \exp(k^2\sigma^2/2). \tag{27}$$

Eq. (24) can often be used to estimate σ for a real log-normal distribution of particle radii, using experimental sizing data, for example from light-scattering[7]. Note that while uniform size and uniform volume

radii distributions are having sharp edges at a_{min} and a_{max}, the log-normal distribution is smoothly increasing and decreasing. Tridisperse maximally equivalent systems to polydisperse ones with log-normal radii distribution, considered in this report in Fig. 2, are detailed in Table 3. Note that the number fraction n_1 of large species decreases very fast with increasing σ. This means that to have in the system, e.g., more than 10 large particles for $\sigma = 1$, one has to use large total numbers of particles $N \geq 10^6$ (no data shown), which is computationally expensive.

Table 3 Specification of tridisperse mixtures of hard spheres maximally equivalent to polydisperse systems with log-normal distribution of radii for various σ.

σ	n_1	n_2	δ_1	δ_2
0.05	0.1330	0.6620	0.1457	0.6653
0.1	0.1040	0.6480	0.1263	0.6611
0.15	0.07972	0.6255	0.1083	0.6543
0.2	0.05980	0.5952	0.09197	0.6448
0.25	0.04384	0.5585	0.07722	0.6329
0.3	0.03138	0.5167	0.06405	0.6186
0.35	0.02190	0.4713	0.05245	0.6021
0.4	0.01488	0.4238	0.04236	0.5836
0.45	0.009833	0.3758	0.03371	0.5634
0.5	0.006306	0.3285	0.02639	0.5416
0.55	0.003918	0.2832	0.02032	0.5186
0.6	0.002355	0.2407	0.01535	0.4945
0.65	0.001367	0.2017	0.01137	0.4695
0.7	0.0007643	0.1666	0.008247	0.4440
0.75	0.0004110	0.1357	0.005847	0.4180
0.8	0.0002121	0.1090	0.004046	0.3920
0.85	0.0001048	0.08627	0.002729	0.3659
0.9	0.00004951	0.06731	0.001792	0.3401
0.95	0.00002231	0.05177	0.001143	0.3147
1.0	0.000009572	0.03923	0.0007078	0.2899

Figure 2 shows the maximum density $\nu_{\max}$ as a function of σ for systems with log-normal radii distribution and for their tridisperse maximal equivalents (with rattlers). A relatively fast compression rate, $\Gamma = 16 \times 10^{-3}$ was used to achieve these configurations, i.e., a monodisperse system (with $\sigma = 0$) does not crystallize and reaches a random close packing. From our data, the jamming density $\nu_{\max}$ can be fitted by a function of σ:

$$\nu_{\max}(\sigma) = \nu_{\max}^{\infty} - (\nu_{\max}^{\infty} - \phi_{\mathrm{RCP}}) \exp(-2\sigma^2), \tag{28}$$

where the random close packing density $\phi_{\mathrm{RCP}} = \nu_{\max}(0)$ is 0.6373 (taken from data) and the maximum density, $\nu_{\max}^{\infty} = 0.7990$, in the limit of $\sigma \to \infty$. Note that Eq. (28) has a similar form as previously reported equations for the jamming density for the uniform size and uniform volume radii distributions[9], i.e.,

$$\nu_{\max}(x) = \nu_{\max}^{\infty} - (\nu_{\max}^{\infty} - \phi_{\mathrm{RCP}})F(x). \tag{29}$$

Based on this observation, we speculate that this is a general form for the jamming density of some large class of polydisperse radii distributions, where a function $F(x)$ can be expressed in terms of moments of the size distribution. Particularly, for the log-normal radii distribution $F(x)$ can be expressed as (this is an arbitrary choice out of many):

$$F_{\ln}(\sigma) \equiv \exp(-2\sigma^2) = \left(\frac{D_{32}}{D_{43}}\right)^2. \tag{30}$$

The deviation of Eq. (28) is within $\pm 0.7\%$ for all data $0 \leq \sigma \leq 1$.

Nevertheless, we found that the jamming density for the log-normal radii distribution can also be fitted by another function, which is very close to Eq. (28) in the range $0 \leq \sigma \leq 1$, but differs for larger σ:

$$\nu_{\max}(\sigma) = \nu_{\max}^{\infty} + c_1 \exp(-\sigma^2) + c_2 \exp(-\sigma^3), \tag{31}$$

with $\nu_{\max}^{\infty} = 0.8583$, $c_1 = -0.3516$ and $c_2 = 0.1332$. The deviation of Eq. (31) is within $\pm 0.4\%$ for all data $0 \leq \sigma \leq 1$.

In Figure 1 we show final snapshots (near jamming) of polydisperse systems and their maximally equivalent tridisperse ones, which are considered in the paper in Figure 2.

3 Measuring bond-orientational order

In order to distinguish particles that are part of the crystal from those that belong to fluid or glass we utilize a method which is independent of the specific crystal structure and does not require the definition of the reference frame (i.e., rotationally invariant), provided by the following algorithm based on spherical harmonics[10–12]. The idea is to calculate for each particle i a set of complex numbers

$$\bar{q}_{lm}(i) = \frac{1}{N_b(i)} \sum_{j=1}^{N_b(i)} Y_{lm}(\hat{\mathbf{r}}_{ij}), \tag{32}$$

where Y_{lm} are spherical harmonics with components m ranging from $-l \leq m \leq l$, evaluated for the normalized direction vector $\hat{\mathbf{r}}_{ij}$ connecting the centers of mass of particles i and j. The components of $\bar{q}_{lm}(i)$ depend on the relative orientation of particle i with respect to its $N_b(i)$ neighboring particles[13]. For determining neighboring particles we utilize a weighted Delaunay tessellation[14] (otherwise called regular triangulation), effectively taking in account radii of particles. These triangulations provide information about inter-particle distances among a set of spheres. The CGAL external library was used for the construction of the triangulation. In order to account for periodic boundaries, we periodically repeat the simulation box in all three directions. We use $l = 6$ because it allows to detect hcp clusters and clusters with cubic symmetry (fcc, bcc, and sc) but also clusters with icosahedral symmetry, which can have nonzero spherical harmonics only for $l = 6, 10, 12, \ldots$[10]. To this end, we construct a normalized complex vector $\mathbf{q}_6(i)$, with components $\tilde{q}_{6m}(i)$ proportional to the $\bar{q}_{6m}(i)$.

In a second step a dot product of the vectors $\mathbf{q}_6$ of neighboring particles i and j is computed:

$$d_6(i,j) = \mathbf{q}_6(i) \cdot \mathbf{q}_6(j) \equiv \sum_{m=-6}^{6} \tilde{q}_{6m}(i) \tilde{q}_{6m}(j)^*, \tag{33}$$

where the * indicates complex conjugation. Here, $d_6(i,j)$ is a normalized quantity correlating the local environments of neighboring particles[13]; it is a real number and is defined in the range $-1 \leq d_6(i,j) \leq 1$. By construction, $d_6(i,i) = 1$. For example[13], in a perfect face-centered-cubic crystal, all the particles have the same environment and, therefore, the dot product between the vectors associated with any pair of particles is unity. The dot product decreases when thermal vibrations are present but, on average, it is close to unity if particles have a solid-like environment and around zero if particles have a liquid-like environment.

Now particles i and j are considered to be "connected" if $\mathbf{q}_6(i) \cdot \mathbf{q}_6(j)$ exceeds a certain threshold, in our case 0.65. A particle is labeled as solid-like if it has at least six connections. Finally, we define the degree of crystallinity p_c, or simply *crystallinity*, of a sample as the number of solid-like particles divided by the total number N.

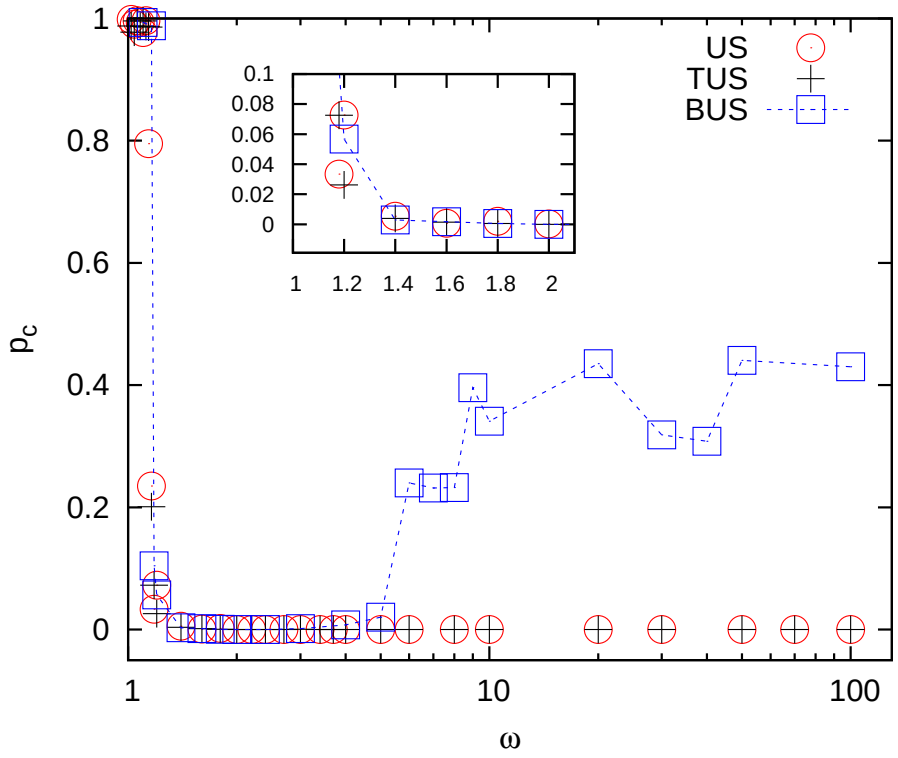

Figure 3 (Color online) Crystallinity plotted against ω for systems with uniform size distribution (US), for their maximally equivalent tridisperse systems (TUS), and for equivalent bidisperse systems (BUS) previously considered[9]. In the inset we zoom into the low ω behavior using the same axis and symbols.

Figure 3 shows the crystallinity p_c as function of size ratio ω for systems with uniform size distribution characterized by its extreme size ratio ω and for their maximally equivalent tridisperse systems (see Sec.2 for details) as well as for equivalent bidisperse systems considered in previous study[9]. Crystallinity data

show that maximally equivalent tridisperse systems do not show any signs of crystallization for $\omega \geq 1.4$, while equivalent bidisperse systems partially crystallize for $\omega > 5$.

4 Structure factor and spectral density

Recently S. Torquato and colleagues[15] have studied the small wavenumber k behavior of the structure factor $S(k)$ of over-compressed amorphous hard sphere configurations for a wide range of densities up to the maximally random jammed state. They have found that a precursor to the glassy jammed state was evident long before the jamming density was reached as measured by a growing nonequilibrium length scale extracted from the volume integral of the direct correlation function. Their results are extended to different systems and to mixtures[16]. While the structure factor $S(k)$ measures local-*number*-density fluctuations, local-*volume*-fraction fluctuations provide the appropriate structural description of non-monodisperse packings because they account correctly for the size distribution of the particles. The analog of the structure factor in this context is the so-called *spectral density*, $\xi(k)$. We investigate if the polydisperse and the respective maximally equivalent tridisperse $S(k)$ and $\xi(k)$ are equivalent too.

Both structure factor and spectral density are numerically obtained using discrete Fourier transforms[17] according to

$$S(\mathbf{k}) = \frac{\left|\sum_{j=1}^{N} \exp(-i\mathbf{k}\cdot\mathbf{r}_j)\right|^2}{N} \quad (\mathbf{k} \neq 0), \text{ and} \tag{34}$$

$$\xi(\mathbf{k}) = \frac{\left|\sum_{j=1}^{N} \exp(-i\mathbf{k}\cdot\mathbf{r}_j)\hat{m}(\mathbf{k};R_j)\right|^2}{V} \quad (\mathbf{k} \neq 0), \tag{35}$$

where

$$\hat{m}(\mathbf{k};R_j) \equiv \int_{\mathbb{R}^d} \exp(-i\mathbf{k}\cdot\mathbf{r})\Theta(R - \|\mathbf{r}\|)d\mathbf{r}, \tag{36}$$

is the Fourier transform of the indicator function for a d-dimensional sphere of radius R. Note that the shape of the domain, defined by a set of lattice vectors $\{\boldsymbol{\lambda}_i\}$, restricts the wave vectors such that $\mathbf{k}\cdot\boldsymbol{\lambda}_i = 2\pi n$ for all i, where $n \in \mathbb{Z}$. To obtain spherically symmetric forms of the structure factor and spectral density, we angularly average over all wave vectors within a spherical shell of thickness $2\pi/\|\boldsymbol{\lambda}_i\|$ in reciprocal space. The wave number k is the magnitude of the wave vector $\mathbf{k}$, i.e., $k = \|\mathbf{k}\|$.

Figures 4, 5, 6, 7 show the structure factor $S(k)$ and the spectral density $\xi(k)$ for several polydisperse systems with uniform size and uniform volume radii-distributions, and for their maximally equivalent tridisperse systems (with rattlers). ($D = 2\langle a \rangle$ is an effective length scale, taken here to be the average diameter.) An exhaustive study of these quantities is well beyond the scope of the present study. Nevertheless, we observe that for low $\omega \leq 3$ the polydisperse and the respective maximally equivalent tridisperse $S(k)$ and $\xi(k)$ are in good agreement for all k-values. With increasing ω the agreement gets worse for high k-values, but still the low k behavior is similar, especially in the case of the uniform size distribution. This observation confirms that maximally equivalent systems are indeed very similar in their microstructure.

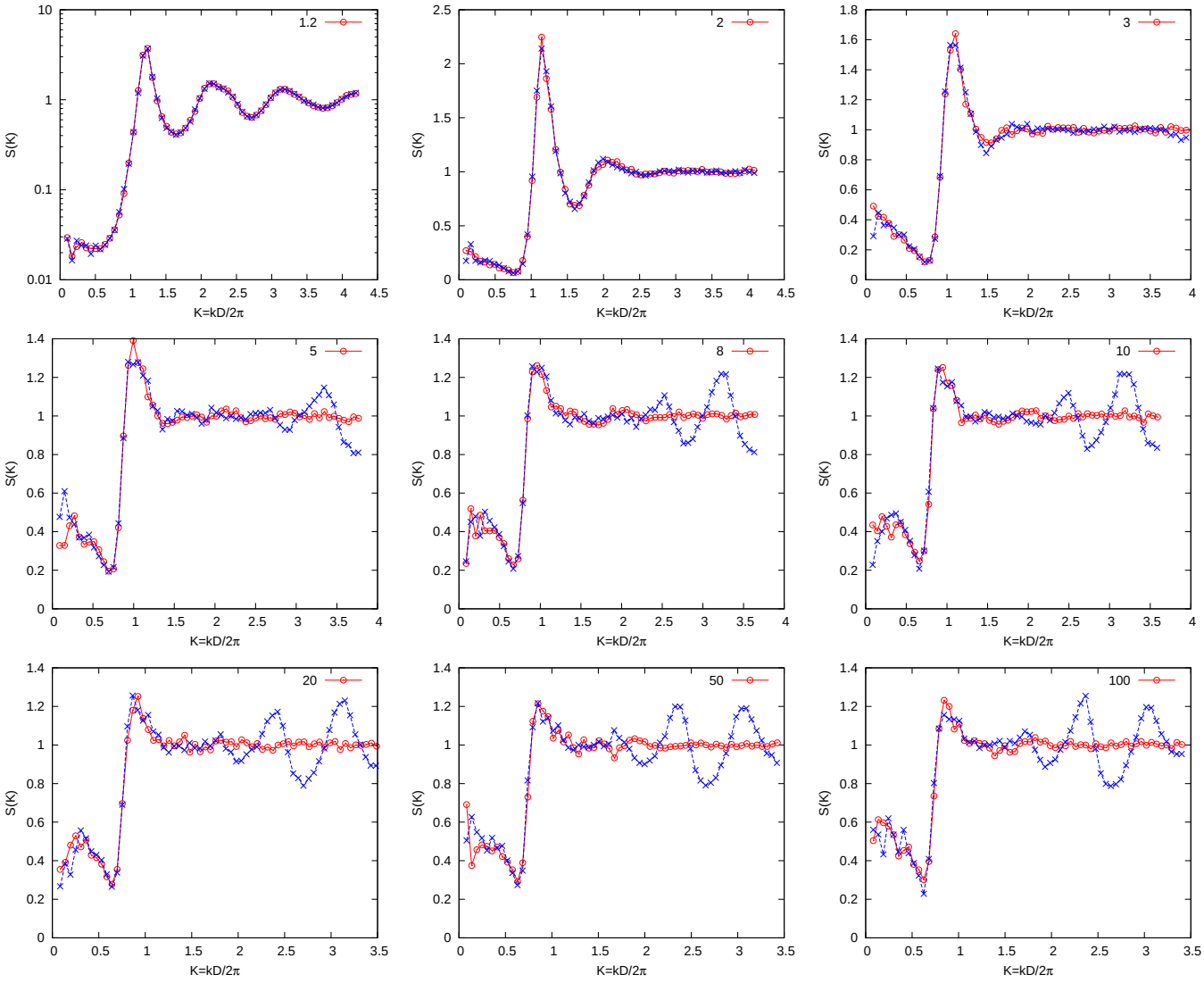

Figure 4 Structure factor as function of the scaled wavenumber for systems with uniform size distribution (circles) and for respective maximally equivalent tridisperse systems (crosses) for different ω given in the insets.

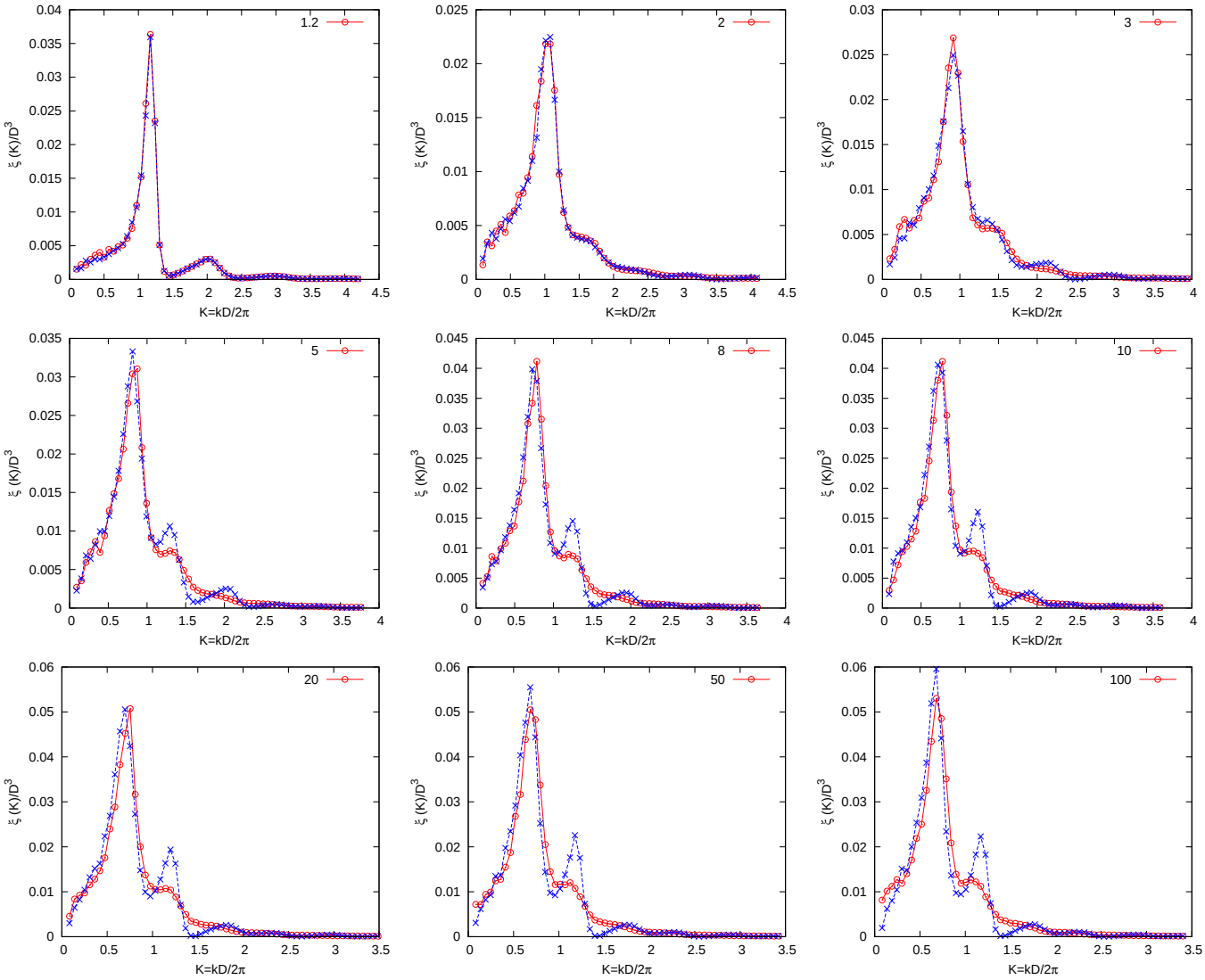

Figure 5 Spectral density as function of the scaled wavenumber for systems with uniform size distribution (circles) and for respective maximally equivalent tridisperse systems (crosses) for different ω given in the insets.

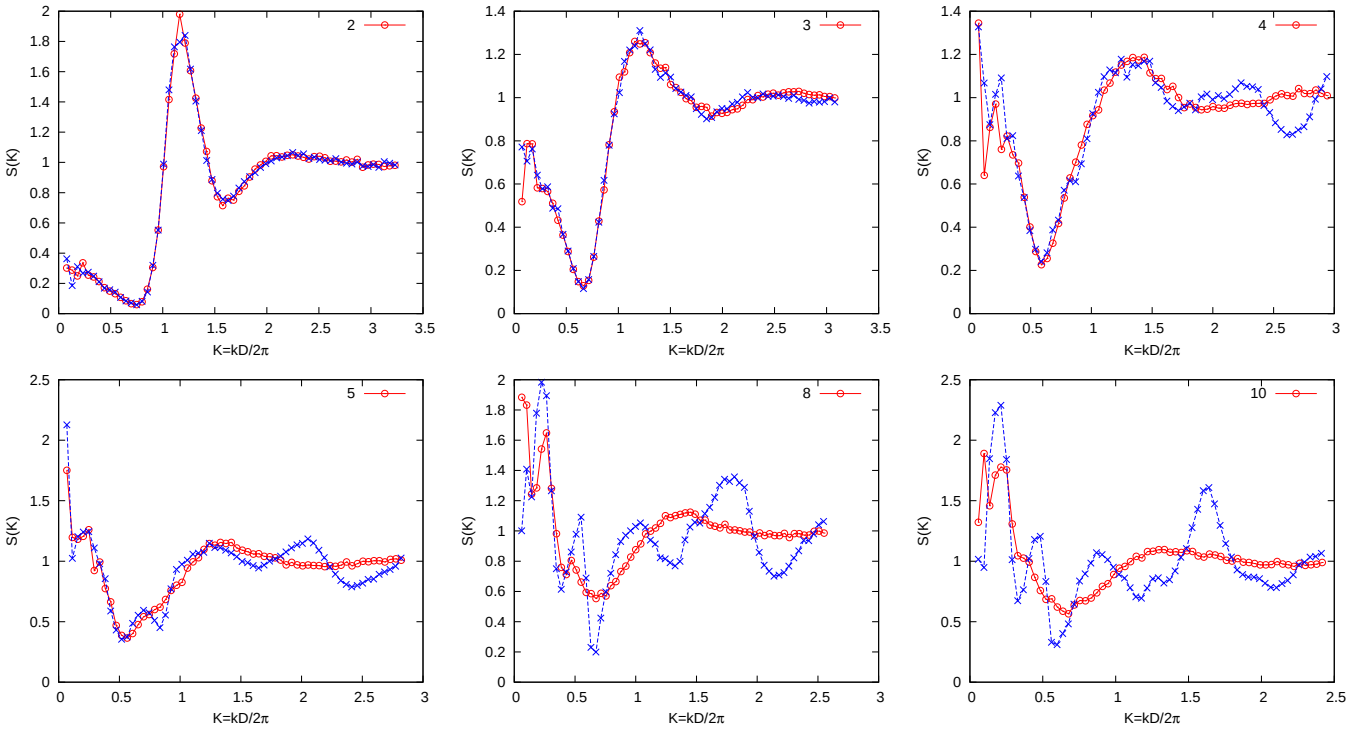

Figure 6 Structure factor as function of the scaled wavenumber for systems with uniform volume distribution (circles) and for respective maximally equivalent tridisperse systems (crosses) for different ω given in the insets.

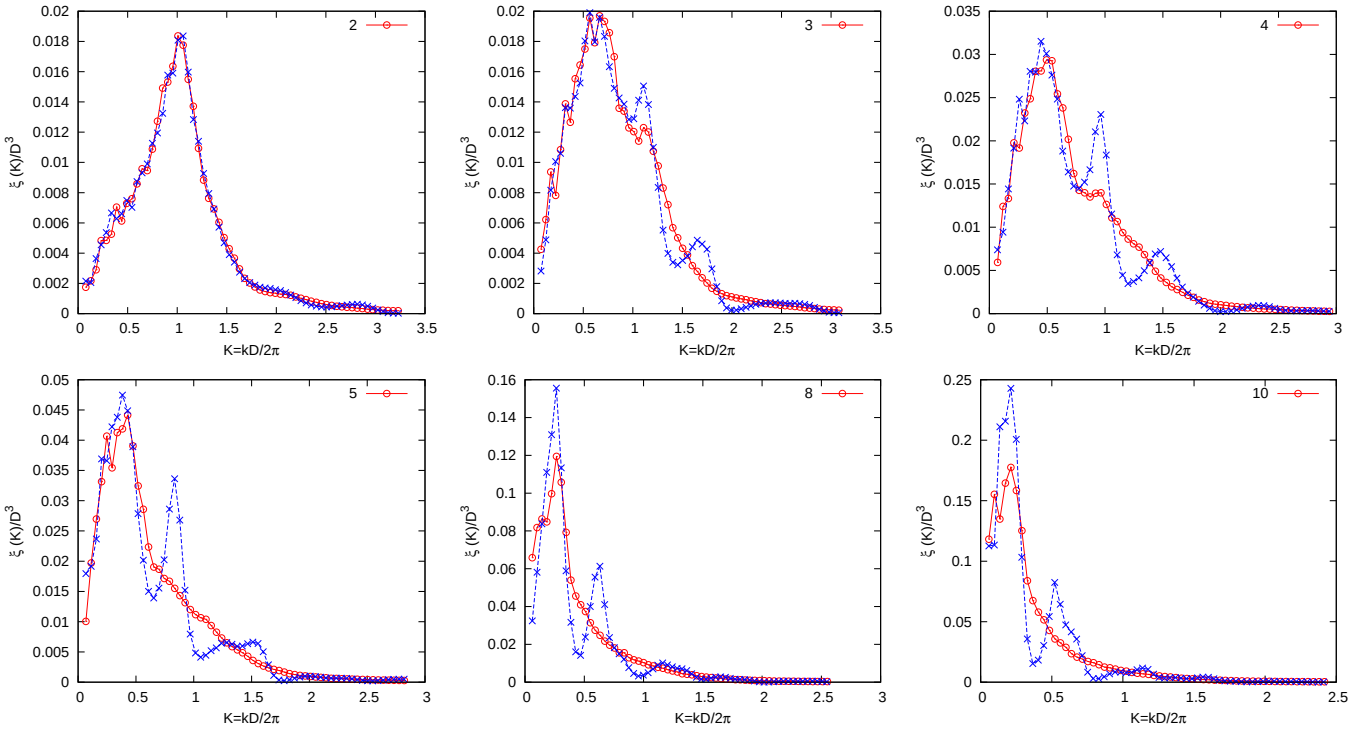

Figure 7 Spectral density as function of the scaled wavenumber for systems with uniform volume distribution (circles) and for respective maximally equivalent tridisperse systems (crosses) for different ω given in the insets.

References

[1] A. Donev, S. Torquato, and F. H. Stillinger, *J. Comput. Phys.*, 2005, **202**(2), 737–764.
[2] M. Skoge, A. Donev, F. H. Stillinger, and S. Torquato, *Phys. Rev. E*, 2006, **74**(4), 041127.
[3] A. Donev, *Jammed Packings of Hard Particles* Ph.d. thesis, Princeton University, 2006.
[4] S. Luding, Collisions & contacts between two particles. In: H. J. Herrmann, J. P. Hovi, S. Luding (eds) Physics of dry granular media - NATO ASI Series E350, Kluwer Academic Publishers, Dordrecht, 1998, 285.
[5] P. Bartlett, *J. Chem. Phys.*, 1997, **107**(1), 188–196.
[6] A. Clauset, C. R. Shalizi, M. E. J. Newman, Power-law distributions in empirical data, *SIAM Review*, 2009, **51**(4), 661–703
[7] R. S. Farr, Random close packing fractions of lognormal distributions of hard spheres, *Powder Technology*, 2013, **245**, 28–34.
[8] J. Söderlund, L. B. Kiss, G. F. Niklasson, and C. G. Granqvist, *Phys. Rev. Lett.*, 1998, **80**(11), 2386–2388.
[9] V. Ogarko, and S. Luding, *J. Chem. Phys.*, 2012, **136**(12), 124508.
[10] P. J. Steinhardt, D. R. Nelson, M. Ronchetti, Bond-orientational order in liquids and glasses, *Phys. Rev. B*, 1983, **28**(2), 784–805.
[11] P. R. ten Wolde, M. J. Ruiz-Montero, and D. Frenkel, *Phys. Rev. Lett.*, 1995, **75**, 2714–2717.
[12] P. R. ten Wolde, M. J. Ruiz-Montero, and D. Frenkel, *Faraday Discussions*, 1996, **104**, 93–110.
[13] P. N. Pusey, E. Zaccarelli, C. Valeriani, E. Sanz, W. C. K. Poon, and M. E. Cates, *Phil. Trans. R. Soc. A*, 2009, **367**(1909), 4993–5011.
[14] L. Pournin *On the behavior of spherical and non-spherical grain assemblies, its modeling and numerical simulation* Ph.d. thesis, École Polytechnique Fédérale de Lausanne, 2005.
[15] A. Hopkins, F. H. Stillinger, and S. Torquato, *Phys. Rev. E*, 2012, **86**, 021505.
[16] E. Marcotte, F. H. Stillinger, and S. Torquato, *J. Chem. Phys.*, 2013, **138**, 12A508.
[17] C. E. Zachary, Y. Jiao, and S. Torquato, *Phys. Rev. Lett.*, 2011, **106**(17), 178001.